EBioMedicine xxx (2015) xxx–xxx

Contents lists available at ScienceDirect

EBioMedicine

journal homepage: www.ebiomedicine.com

Selective Impairment of Spatial Cognition Caused by Autoantibodies to the N-Methyl-D-Aspartate Receptor

Eric H. Chang [a,1], Bruce T. Volpe [b,g,1], Meggan Mackay [c,1], Cynthia Aranow [c], Philip Watson [d], Czeslawa Kowal [c], Justin Storbeck [d], Paul Mattis [e], RoseAnn Berlin [b], Huiyi Chen [f], Simone Mader [c], Tomás S. Huerta [a], Patricio T. Huerta [a,c,g,2], Betty Diamond [c,g,*,2]

[a] Laboratory of Immune & Neural Networks, Feinstein Institute for Medical Research, North Shore LIJ Health System, Manhasset, NY 11030, USA
[b] Laboratory of Functional Neuroanatomy, Feinstein Institute for Medical Research, North Shore LIJ Health System, Manhasset, NY 11030, USA
[c] Autoimmune & Musculoskeletal Disease Center, Feinstein Institute for Medical Research, North Shore LIJ Health System, Manhasset, NY 11030, USA
[d] Department of Psychology, Queens College, Flushing, NY 11367, USA
[e] Susan and Leonard Feinstein Center for Neurosciences, Feinstein Institute for Medical Research, North Shore LIJ Health System, Manhasset, NY 11030, USA
[f] School of Biological Sciences, Lee Kong Chian School of Medicine, Nanyang Technological University, Singapore 637551, Singapore
[g] Department of Molecular Medicine, Hofstra North Shore-LIJ School of Medicine, Manhasset, NY 11030, USA

ARTICLE INFO

Article history:
Received 8 April 2015
Received in revised form 26 May 2015
Accepted 27 May 2015
Available online xxxx

Keywords:
Lupus
Neuropsychiatric lupus
CA1 place cell
Hippocampus
Mouse lupus model

ABSTRACT

Patients with systemic lupus erythematosus (SLE) experience cognitive abnormalities in multiple domains including processing speed, executive function, and memory. Here we show that SLE patients carrying antibodies that bind DNA and the GluN2A and GluN2B subunits of the N-methyl-D-aspartate receptor (NMDAR), termed DNRAbs, displayed a selective impairment in spatial recall. Neural recordings in a mouse model of SLE, in which circulating DNRAbs penetrate the hippocampus, revealed that CA1 place cells exhibited a significant expansion in place field size. Structural analysis showed that hippocampal pyramidal cells had substantial reductions in their dendritic processes and spines. Strikingly, these abnormalities became evident at a time when DNRAbs were no longer detectable in the hippocampus. These results suggest that antibody-mediated neurocognitive impairments may be highly specific, and that spatial cognition may be particularly vulnerable to DNRAb-mediated structural and functional injury to hippocampal cells that evolves after the triggering insult is no longer present.

1. Introduction

The autoimmune disease systemic lupus erythematosus (SLE) affects multiple organs; most organ damage is initiated by autoantibody deposition that triggers subsequent inflammatory reaction (Tsokos, 2011). Neuropsychiatric lupus (NPSLE) refers to the neurologic manifestations of SLE that are present in 30–80% of patients (Nowicka-Sauer et al., 2011). These symptoms develop insidiously, cause disability, and significantly diminish quality of life (Appenzeller et al., 2009). Impaired cognition is reported frequently in clinically stable SLE patients that do not have other NPSLE manifestations or inflammation in the central nervous system (CNS) (Toledano et al., 2013). Despite the high prevalence of cognitive dysfunction and emotional disturbance in NPSLE patients, the wide array of symptoms attributable to NPSLE has hampered mechanistic understanding.

When DNRAbs access the brain through a damaged blood–brain barrier (BBB) (Hirohata et al., 2014), they are likely to cause non-focal CNS manifestations of NPSLE (reviewed in Diamond et al., 2013). Notably, DNRAbs have been extracted from brain tissue of SLE patients (Kowal et al., 2006) and elevated DNRAb titers in cerebrospinal fluid (CSF) associate with NPSLE symptoms (Arinuma et al., 2008; DeGiorgio et al., 2001; Lauvsnes and Omdal, 2012; Yoshio et al., 2006). DNRAbs bind a consensus sequence (D/E W D/E Y S/G, or DWEYS for short) present in the extracellular domains of the GluN2A and GluN2B subunits

Abbreviations: AP, alkaline phosphatase; BBB, blood–brain barrier; BDI, Beck depression index; CA1, *cornus ammonis* area 1 of the hippocampus; CNS, central nervous system; CSF, cerebrospinal fluid; C3, C4, complements 3 and 4, respectively; DMARD, disease-modifying drugs; DNRAb, anti-DNA antibody reactive to the GluN2A and GluN2B subunits of the NMDAR; dsDNA, double stranded DNA; DWEYS, amino acid consensus sequence (D/E, W, D/E, Y, S/G) for DNRAb binding; FA, Freund's adjuvant; HC, healthy control; HEK-293T, human embryonic kidney 293 T cell; IgG, immunoglobulin G; i.p, intraperitoneally; LPS, lipopolysaccharide; MAP, multi-antigenic polylysine backbone; NMDAR, N-methyl-D-aspartate receptor; NOR, novel object recognition; NPSLE, neuropsychiatric lupus; OPM, object place memory; SELENA, safety of estrogens in lupus erythematosus national assessment; SLE, systemic lupus erythematosus; SLEDAI, systemic lupus erythematosus disease activity index; SLICCDI, systemic lupus international collaborating clinics damage index.

* Corresponding author at: Center of Autoimmune & Musculoskeletal Disease, Feinstein Institute for Medical Research, 350 Community Drive, Manhasset, NY 11030, USA.
E-mail address: bdiamond@nshs.edu (B. Diamond).
[1] Co-first author.
[2] Co-senior author.

http://dx.doi.org/10.1016/j.ebiom.2015.05.027

(Paoletti, 2011). Mechanistic studies show that DNRAbs preferentially bind the open configuration of the NMDAR, augment NMDAR-mediated synaptic potentials, and, at higher concentration, trigger mitochondrial stress and apoptosis through binding specifically to GluN2A-containing NMDARs (Faust et al., 2010). DNRAbs that have been isolated from serum of SLE patients and intravenously transferred to mice lead to death of hippocampal neurons and impaired memory flexibility after the mice are given lipopolysaccharide (LPS) to impair the integrity of the BBB within the hippocampus (Kowal et al., 2006).

We have developed an in vivo model in which BALB/c mice synthesize DNRAbs following immunization with a configuration of the consensus sequence multimerized on a polylysine backbone (termed MAP-DWEYS), while BALB/c mice immunized with the polylysine backbone alone (MAP-core) do not (Kowal et al., 2004). This model allows us to evaluate DNRAbs as causal agents of neuronal injury, independent of other autoantibodies and the high levels of systemic inflammatory mediators found in spontaneous mouse SLE models (Sakic, 2012). Circulating DNRAbs cause no detectable brain pathology in MAP-DWEYS immunized mice with an intact BBB. However, upon exposure to LPS, mice have 20–25% loss of hippocampal neurons (occurring within the first week post-LPS) and persistent memory impairment, assessed in the T-maze and the Morris water maze (Kowal et al., 2004).

Here we show that SLE patients with high serum titers of DNRAbs exhibit a selective impairment in spatial cognition compared to healthy subjects. Moreover, DNRAbs in mice also lead to a selective spatial memory impairment, associated with functional and structural abnormalities in the surviving hippocampal pyramidal neurons. These alterations evolve after the DNRAbs are no longer detectable in brain tissue and are sustained for months thereafter.

2. Materials and Methods

2.1. Human Subjects

The Institutional Review Board of the North Shore-LIJ Health System and Queens College approved the human study. Informed consent was obtained from all subjects. SLE patients were at least 18 years old, fulfilled the revised criteria for SLE (American College of Rheumatology, 1999), and had stable disease activity and medication doses for 4 weeks prior to screening (Table 1). Exclusion criteria, designed to limit potentially confounding factors, included a history of neuropsychiatric impairment from any cause, cerebrovascular disease, current use of anti-depressant, anti-psychotic or anxiolytic drugs or illicit drug use. Importantly, none of the SLE patients met criteria for any NPSLE manifestations (American College of Rheumatology, 1999). Subjects were recruited from the Rheumatology Clinic at the Feinstein Institute for Medical Research, Jamaica Hospital in Queens, and Lenox Hill Hospital in Manhattan. Healthy control (HC) subjects were recruited through SLE patients that asked their friends to participate and through flyers posted in posted in schools. Disease activity was assessed in all SLE subjects, within 10 days of testing, with the Safety of Estrogens in Lupus Erythematosus National Assessment and Systemic Lupus Erythematosus Disease Activity Index (SELENA; SLEDAI) (Petri et al., 1999), as well as the Systemic Lupus International Collaborating Clinics Damage Index (SLICCDI) (Gladman et al., 1997). Neuropsychological assessment was performed in a quiet room by one investigator (PW) who remained blinded to DNRAb status of patients.

Table 1
Clinical characteristics of SLE patients.

	Healthy control	SLE DNRAb−	SLE DNRAb+	P*
Number	27	27	22	
Age (mean)	38.2 ± 11.6	43.5 ± 9.6	40.5 ± 9.7	0.287
Gender: female	100%	100%	100%	
Ethnicity				
African American	55.6%	77.8%	59.1%	
Caucasian	22.2%	18.5%	13.6%	
Hispanic	14.8%	3.7%	22.7%	
Asian	3.7%	0	4.5%	
Other	1.3%	0	0	
Education (mean)	14.8 ± 1.84	14 ± 2.1	12.8 ± 2.1	0.056
BDI (mean)	2.8 ± 3.2	8.1 ± 6.0	6.2 ± 6.3	0.289
BDI: % with mild, moderate depression	3.7%	25.9%	18.2%	0.518
Disease duration (years)		13.7 ± 8.6	13 ± 9.4	0.772
Medications				
Current prednisone (mg per day)		2.9 ± 4.0	2.5 ± 4.4	0.759
Current DMARD use		59%	48%	0.445
SLEDAI (mean)		1.5 ± 1.7	1.9 ± 1.7	0.422
SLE damage index (mean)		0.85 ± 1.4	1.0 ± 1.2	0.686
Anti-dsDNA antibody titer % high		40.7%	63.6%	0.111
C3 (mean)		109.2 ± 24.7	99.1 ± 33.4	0.23
C4 (mean)		24.0 ± 11.0	17.7 ± 9.7	0.042
Anti-Ro antibody		48.1%	54.5%	0.656
Anti-ribosomal P antibody		14.8%	13.6%	0.907
ACL antibody (IgG or IgM)		0	4.5%	0.263

Data are mean ± SEM, except where otherwise indicated. There were no clinical differences between the DNRAb+ and DNRAb− groups in areas that may have confounded results of the cognitive task including age, education, disease activity, disease duration, depression, medication use and other autoantibodies. * *P* values represent comparisons, by *t* test, between the two SLE groups.

2.2. Animals and Behavioral Assessments

The Feinstein Institute Animal Care and Use Committee approved all animal procedures. Female BALB/cJ mice (Jackson Labs, 8 weeks old) were immunized, intraperitoneally (i.p.), with 100 μg (in 100 μL of saline) of MAP-DWEYS (DNRAb+ group, $n = 10$), or with the MAP-core polylysine backbone (DNRAb− mice, $n = 10$), in complete Freund's adjuvant (FA), and twice more in incomplete FA as previously described (Kowal et al., 2004). The animals for each group were chosen randomly, based on litter. LPS (3 mg per kg) diluted in lactated Ringers (*Escherichia coli*, 055:B5, Sigma-Aldrich, St. Louis, MO) was i.p. injected twice, 48 h apart, at 4 weeks after the last immunization. Behavioral assessments were conducted during the dark (active) cycle. Mice were initially subjected to the object place memory (OPM) task (Faust et al., 2013) and then the novel object recognition (NOR) task (Chang and Huerta, 2012). Mice were maintained on a reverse schedule of 12 h of darkness (07:00 to 19:00) and 12 h of light, with ad libitum access to food and water. Starting one week before testing, mice were handled for 5 days in daily sessions of 5 to 10 min. Handling and subsequent experiments were conducted during the dark period of their circadian cycle. Investigators (TSH and PTH) were blinded to group allocation during the experiments, but not during data analysis.

For the OPM task (Faust et al., 2013), the apparatus consisted of a chamber with a square base (40 cm on the side) and 60-cm high walls built of polyvinyl chloride. Three walls were opaque with black inserts, while the fourth wall was transparent. A light bulb (50 W) of orange hue illuminated the chamber from above. An infrared-sensitive camera above the chamber was connected to the video input of the behavioral tracking software (Ethovision XT8.5, Noldus, Wageningen, Netherlands), which recorded the animal's position at 30 frames per second. DNRAb+ ($n = 10$) and DNRAb− mice ($n = 10$) were transported inside their home cages into the darkened experimental room and placed in the empty chamber, one at a time, for 4 sessions (2 per day) of 15 min. On the third day, mice were subjected to the OPM task, which consisted of a familiarization trial (T1), a sample trial (T2), and a choice trial (T3), interspersed by 10-min delays that were spent in a highly habituated holding chamber. For T1, animals were placed in the empty chamber for 15 min. For T2, mice explored the chamber for 5 min in the presence of two identical objects, which were located in 2 of 4 possible sites at the center of the NW, NE, SW or SE quadrants of the chamber. For T3, which lasted 5 min, one object (chosen at random) remained in the

Please cite this article as: Chang, E.H., et al., Selective Impairment of Spatial Cognition Caused by Autoantibodies to the N-Methyl-D-Aspartate Receptor, EBioMedicine (2015), http://dx.doi.org/10.1016/j.ebiom.2015.05.027

familiar position while the second object was moved to a location that was the center of the adjacent quadrant, 20 cm apart from its previous position. Object exploration was measured with a software algorithm (Ethovision) that assigned a circular zone (diameter, 6.5 cm) around each object and recorded the episodes in which the animal's snout was in close proximity (<1 cm) to the object's periphery. We have previously validated software-based methods for animal tracking (Chang and Huerta, 2012). The number of visits and the times spent exploring each object on T2 and T3 were used for statistical comparisons. For T2, an exploration ratio was defined as the time exploring the right object (in either NE or SE zone) divided by the sum of the times exploring both objects. For T3, an OPM ratio was defined as the time exploring the moved object minus the time exploring the stable object over the sum of the times exploring both objects.

For the NOR task (Chang and Huerta, 2012), the apparatus consisted of a chamber with a square base (30 cm on the side) and 80-cm high walls made of white polyvinyl chloride. Each mouse had 4 familiarization sessions to insure full acclimation to the context. The NOR task consisted of a sample trial (5 min), followed by delay (10 min), and a choice trial (5 min). For the sample trial, mice explored the chamber in the presence of two identical objects. After the delay, mice were returned to the experimental chamber for a choice trial in which they explored a triplicate copy of the sample object and a fresh object (never encountered before). The number of visits and the times spent exploring each object on sample and choice trials were used for statistical comparisons. For choice trials, an NOR ratio was defined as the time exploring the novel object minus the time exploring the familiar object over the sum of the times exploring both objects.

2.3. Biochemical Assays

The hippocampus was extracted from DNRAb + and DNRAb − mice and ELISAs were performed for immunoglobulin G (IgG), albumin and anti-DWEYS antibodies. In brief, both hippocampi were extracted from perfused brain and a lysate was made by sonication using a 20:1 ratio of lysis buffer to brain tissue followed by centrifugation (10,000 rpm, 30 min, 4 °C). For IgG, Costar half-volume plates (3690, Corning, Tewksbury, MA) were coated with goat anti-mouse IgG (5 μg per mL, Southern Biotech, Birmingham, AL) in $NaHCO_3$ (0.1 M, pH 8.6) overnight at 4 °C. Following blocking with BSA/PBS (1%, 1 h, 37 °C), the lysate and IgG standard (Southern Biotech) were incubated in BSA/PBS (0.2%, 1 h, 37 °C). After PBS-Tween wash, alkaline phosphatase (AP)-linked anti-mouse IgG (Southern Biotech) was added to BSA/PBS (0.2%, 1 h, 37 °C) followed by AP substrate (Sigma-Aldrich).

For albumin, the Costar 3690 plates were coated with goat anti-mouse albumin antibody (1 μg per mL, Bethyl, Montgomery, TX) in $NaHCO_3$ (0.1 M, pH 8.6) overnight at 4 °C. The plates were processed as above and incubated with albumin standard and lysates (1 h, 37 °C), followed by incubation with goat anti-mouse albumin-biotinylated antibody (Bethyl) at 1:2000 dilutions (1 h, 37 °C). The plates were washed again with PBS-Tween, incubated with AP-conjugated streptavidin (SA, 1:2000 dilution, Southern Biotech) for 20 min at RT, and developed with AP substrate.

ELISA for DWEYS was done in Costar 3690 plates (Corning) that were dry coated with unlabeled SA (30 μg per mL, Southern Biotech) in $NaHCO_3$ (0.1 M, pH 8.6) overnight at 37 °C. The plates were blocked with BSA/PBS (1%, 1 h, RT) with gentle shaking, washed 1× with PBS-0.05% Tween, and incubated with C-terminal biotinylated DWEYS (5 μg per mL, GenScript, Piscataway, NJ) in BSA/PBS (0.2%, 1 h, RT) with shaking. They were washed 6× with PBS-T followed by incubating brain lysates in BSA/PB (0.2%, 1.5 h at RT, or overnight at 4 °C). The plates were washed with PBS-T, incubated with AP-conjugated goat anti-mouse IgG (1:2000, Southern Biotech) in BSA/PBS (0.2%, 1 h at RT) with shaking, and developed with AP substrate.

To detect anti-DWEYS antibody in human serum, plates were coated with the peptide, DWEYSVWLSN as described in Kowal et al. (2006). Serum was tested for DWEYS binding at a 1:100 dilution. Normal values were determined using 20 unselected control sera, within a 2 SD range. HC sera were all within the normal range.

Real-time PCR was performed in hippocampal tissue from perfused brains that were homogenized in Trizol (Life Technologies, Carlsbad, CA). The RNA was purified according to manufacturer's protocol, and it was DNase-treated (DNA-free DNA removal kit AM1906, Invitrogen). Reverse transcription was performed with Superscript III (Invitrogen), whereas real-time PCR was run with Roche's LightCycler 480 Probes Master mix and Nos2 Taqman probe (Mm00440502_m1) on a LightCycler 480 II instrument (Roche, Basel, Switzerland). The results were normalized by Polr2a probe (Mm00839493_m1).

2.4. Antibody Binding to Live Cells

Human embryonic kidney 293 T (HEK-293 T) cells were used for this study. Human monoclonal antibodies G11 (DNRAb) and B1 (non-NMDAR reactive) were analyzed for binding to the NMDAR on the cell membrane of doubly transfected HEK-293 T cells (either GluN1–GluN2A or GluN1–GluN2B), using a modified live cell-based immunofluorescence assay (Mader et al., 2010). HEK-293 T cells transfected with GluN2A or GluN2B alone did not exhibit cell-surface expression of GluN2A or GluN2B protein. Cells were cultured in 96-well tissue culture plates in Dulbecco's modified Eagle's medium (DMEM, Invitrogen, Waltham, MA) with fetal bovine serum (FBS, 10%), penicillin (50 IU per mL), streptomycin (50 mg per mL), L-glutamine (2 mM), and MK801 (10 μM, Tocris, Bristol, UK). After 24 h, cells were transfected with lentiviral expression plasmids for human full-length *Grin1* (GluN1), together with *Grin2A* (GluN2A), or *Grin2B* (GluN2B), at a 1:1 ratio (GluN1–GluN2A or GluN1–GluN2B) using HD Transfection reagent according to the manufacturer's instructions (Fugene 6 transfection reagent, Roche). Untransfected cells as well as single transfected cells (GluN1, GluN2A or GluN2B) served as controls. Cells were washed with PBS (10%) supplemented with FBS (10%), and stained with G11 (20 μg per mL) or B1 (20 μg per mL), and simultaneously with rabbit polyclonal antibody directed to the extracellular domain of GluN2A or GluN2B (0.1 μg per mL, Alomone Labs, Jerusalem, Israel). Antibody binding was detected with AlexaFluor 488 conjugated goat anti-human IgG antibody, or Alexa 594 conjugated goat anti-rabbit IgG antibody, for 30 min. Controls included omitting one or both primary antibodies as well as secondary antibodies. To demonstrate that G11 did not bind polyclonal rabbit IgG, we incubated the cells with human monoclonal antibody and rabbit polyclonal Glucose Transporter GLUT2 antibody (Millipore, Billerica, MA) since GLUT2 is abundantly expressed on the cell membrane of HEK-293 T cells.

2.5. Neuronal Recordings in Freely Behaving Mice

Two cohorts of mice were used in these studies; in the first cohort, DNRAb + ($n = 4$) and DNRAb − ($n = 4$) mice were implanted with customized multi-electrode arrays (Chang and Huerta, 2012; Faust et al., 2013) and neural activity was recorded (as described below) before and after LPS treatment, up to 4 weeks post-LPS. In the second cohort, DNRAb + ($n = 4$) and DNRAb − ($n = 3$) mice were initially treated with LPS, were implanted with arrays at 7 weeks post-LPS, and were subjected to neural recordings at 8–9 weeks post-LPS.

Neural activity was recorded via a unitary gain headstage preamplifier (HS-18, Neuralynx Bozeman, MT). Local field potentials were acquired at a sampling rate of 3 kHz and band-pass filtered (0.1 Hz to 500 Hz) by a Lynx-8 programmable amplifier (Neuralynx) on a personal computer running acquisition software (Cheetah, Neuralynx). The same recording system was used to acquire single units at a sampling rate of 30 kHz and band-pass filter between 500 Hz and 9 kHz. Continuous local field potentials and single unit data were analyzed using NeuroExplorer version 3 (NeuroExplorer, Littleton, MA), OfflineLineSorter (Plexon, Dallas, TX), and Spike2 (Cambridge Electronic Design, Cambridge, UK) software packages.

Please cite this article as: Chang, E.H., et al., Selective Impairment of Spatial Cognition Caused by Autoantibodies to the N-Methyl-D-Aspartate Receptor, EBioMedicine (2015), http://dx.doi.org/10.1016/j.ebiom.2015.05.027

Two light-emitting diodes on the implanted electronic interface board were used for tracking the location of the mouse in space at 30 frames per sec by the acquisition software (Cheetah). To analyze single unit activity, putative single units in CA1 were amplitude thresholded and then sorted with principal component analysis followed by manual cluster cutting (OfflineLineSorter). Spike-related parameters such as spike width, amplitude, shape, timing, and rate were used to subsequently categorize units as putative CA1 pyramidal neurons or interneurons. Only CA1 pyramidal neurons were analyzed further. We constructed firing rate maps by calculating the total number of spikes for each pixel and then dividing by the dwell time for a particular session. Place cell field size was calculated as at least 8 contiguous pixels that shared an edge and were at least 20% of the peak-firing rate for that unit. For units displaying more than one place field, the place field size was computed as the sum of the existing fields. Spatial information was calculated by estimating the rate of information I(R|X) between firing rate R and location X according to the formula (Skaggs et al., 1993; Cacucci et al., 2008):

$$I(R|X) \approx \sum_i p\left(\vec{x}_i\right) f\left(\vec{x}_i\right) log_2 \left(\frac{f\left(\vec{x}_i\right)}{F}\right)$$

in which $p(x_i)$ is the probability of the animal being at location x_i; $f(x_i)$ is the firing rate at location x_i; F is the mean firing rate of the cell. The final electrode positions were marked with electrolytic lesions (0.1 mA for 10 s) after the final recording session. Mice were then sacrificed and their brain tissue was processed for Nissl staining. Recording sites were reconstructed using a combination of electrophysiological markers, microdrive movement, and post-mortem histology.

2.6. Structural Analysis of Pyramidal Neurons

For Golgi staining, mice were anesthetized and perfused with heparinized saline and brains were immersed in equal parts of Solutions A and B (FD Neuro Technologies FD Rapid GolgiStain Kit, Ellicott City, MD), with a single solution change within 24 h. After two weeks, brains were transferred into Solution C (2 days at 4 °C). Tissue was blocked and cut on the cryostat in 100-μm sections and mounted onto gelatin-coated microscope slides and stained with solution D. Slides were coverslipped and allowed to dry flat in the dark for two weeks before analysis. To be included in the data analysis of spines or dendritic arborization, a neuron had to include basal dendrites, apical dendrites and a cell body. The arbor needed to be distinguished visually from nearby neurons. For the spine analysis, Z-stack (0.5-μm separation) photomicrographs were taken under 100× oil magnification of the CA1 neurons (Axio-Imager Z-1, Axio-Vision 4.7, Zeiss, Oberkochen, Germany). Images were transferred to a software program (Neurolucida, MBF Bioscience, Williston, VT) that displayed the Z-stack information so that the spines on the dendrites were visualized, identified and counted. The program generated the number of spines per unit length. A similar procedure was employed for dendrite analysis; Z-stack mosaics (0.294 μm^2) were collected, the files were transferred for analysis, and the tracing of the dendritic arbor was quantified by Scholl analysis.

2.7. Statistical Analysis

We used Origin Pro (version 9, OriginLab, Northampton, MA) for all statistical comparisons. ANOVA, Student's t test, and non-parametric tests, such as Kruskal-Wallis ANOVA and Kolmogorov Smirnov test, were used as indicated in the text. $P < 0.05$ was considered statistically significant.

2.8. Role of Funding Sources

This research was funded by NIH grants (P01-AI073693 and P01-AI102852). The funding agency did not have any involvement in the study design, data collection, data analysis, and the interpretation of results, nor in the writing or decision to submit the article.

3. Results

3.1. Impaired Spatial Cognition in SLE patients with DNRAbs

Because patients with elevated CSF titers of DNRAbs exhibit non-focal neuropsychiatric symptoms (Arinuma et al., 2008; Fragoso-Loyo et al., 2008; Gono et al., 2011; Yoshio et al., 2006), we asked whether the failure to reliably identify a neuropsychiatric symptom that associates with elevated serum titers of DNRAbs might reflect a failure to pinpoint the cognitive domain most vulnerable to the autoantibodies. The hippocampus is a critical brain substrate for spatial cognition, and neuroimaging studies have identified it as a pathological site in SLE (Appenzeller et al., 2006; Ballok et al., 2004). Therefore, we asked whether DNRAbs might specifically impair spatial memory. We recruited SLE subjects ($n = 46$), and a cohort of healthy control (HC) subjects ($n = 27$), which were matched for age, sex, race, and education (Table 1). For SLE patients, we used strict inclusion criteria; subjects did not have active disease (flares), had similar disease duration, and lacked a history of psychiatric episodes, neurologic diagnoses, or clinical events that could confound neuropsychological testing. None were currently on anti-depressive medication. DNRAb titers were assayed in all patients and were elevated in 22 of 49 SLE subjects (44%) consistent with the reported incidence observed in previous studies (Hanly et al., 2004).

Standardized batteries of neuropsychiatric assessments do not include a specific test for spatial recall; hence, we implemented a task that assessed both object recognition and memory for spatial relations. Subjects observed drawings of objects (arranged as 2 × 2 arrays) and, immediately after viewing, were asked either an identification question that did not address spatial relations (identification memory) or a question about the spatial arrangement of the array (spatial memory; Fig. 1A). For the former, they were asked whether a particular object was present in the array; for the latter, they were asked about the spatial relation between two objects in the array, i.e., whether an object was located above, below, left, or right of another object. All groups performed comparably in identification memory (Fig. 1B). While DNRAb− patients were comparable to the HC group in the spatial memory task, DNRAb+ patients performed significantly worse than the HC cohort (Fig. 1B). Therefore, the data support the hypothesis that poor spatial performance in DNRAb+ patients is attributable to the presence of those antibodies. Indeed, DNRAb+ patients as a group performed worse than DNRAb− patients in the spatial memory task except for one poor-performing outlier in the DNRAb− cohort (Fig. 1C). It is important to note that the presence of circulating antibodies does not mean they traverse the BBB to cause neuronal injury, which would explain the observations that not all DNRAb+ patients displayed defective spatial memory and that DNRAb titer in serum was poorly correlated with degree of defect (data not shown).

3.2. Selective Impairment of Spatial Memory in DNRAb+ Mice

While we had identified a DNRAb mediated spatial memory impairment in mice (Kowal et al., 2004), we had not shown that spatial memory was selectively vulnerable. Thus, we assessed DNRAb+ and DNRAb− mice given LPS to cause antibody penetration into the hippocampus. At 8-weeks post-LPS, each animal was tested in the OPM task, which measures spatial memory (Faust et al., 2013), and the NOR task in which spatial relations are irrelevant to the exploration on a non-familiar object (Chang and Huerta, 2012). DNRAb+ mice ($n = 10$) had equivalent scores to DNRAb− mice ($n = 10$) in the NOR task (Fig. 2A, $P = 0.83$). In contrast, DNRAb+ mice performed significantly worse than DNRAb− mice in the spatial OPM task (Fig. 2B, $P = 0.006$).

The sustained impairment in spatial memory might result from permanent exposure to DNRAbs, although the integrity of the BBB recovers by 48 h of systemic LPS treatment (Laflamme et al., 2001) and negligible IgG levels occur in the hippocampus by 1 week post-LPS (Kowal et al., 2004). To address the possibility of lingering antibody, we developed a highly sensitive ELISA for DNRAbs and also measured albumin and IgG in the hippocampus at several post-LPS time points. Equivalent amounts of albumin and IgG were present in DNRAb+ and DNRAb− mice and reached negligible levels by 14 days post-LPS (Fig. 2C). In contrast, DNRAb reactivity was detected exclusively in hippocampal tissue of DNRAb+ mice at 24 h and 48 h post-LPS, and it was absent by 2 weeks post-LPS (Fig. 2D). Thus, the impairment in spatial memory was present after specific antibody titers had declined to undetectable levels.

We previously demonstrated by ELISA that DNRAbs bind GluN2A and GluN2B (DeGiorgio et al., 2001). To confirm that the DNRAb-mediated pathology was secondary to the binding of DNRAbs to NMDARs (expressed in the cell membrane), we developed a cell-based assay and showed co-localization of G11 (human monoclonal DNRAb cloned from a SLE patient) and rabbit GluN2A (commercial antibody to GluN2A) in HEK-293 T cells transfected with GluN1 and GluN2A (Fig. 3A). Similarly, there was co-localization of G11 and rabbit GluN2B in HEK-293 T cells transfected with GluN1 and GluN2B (Fig. 3B). To demonstrate that co-localization did not reflect the binding of G11 to rabbit antibody, we stained untransfected HEK-293 T cells with both anti-GLUT2 antibody and G11, and found that G11 did not bind to untransfected cells (Fig. 3C). Thus, DNRAbs cross-react with surface NMDARs containing GluN2A or GluN2B, confirming that the effects of DNRAbs are mediated through NMDARs.

3.3. Expansion of Place Fields in CA1 Place Cells of DNRAb + Mice

We sought to understand the neural substrate of the spatial impairment caused by DNRAbs. It is well known that pyramidal neurons in the CA1 region of the hippocampus display place cell activity, such that an individual neuron fires intensely within a given area and remains silent in the rest of the environment. The area of neuronal firing is termed the place field (O'Keefe, 2007). Place fields are responsible for the formation of spatial maps and show a maturation process that is dependent on NMDARs (Ekstrom et al., 2001; Kentros et al., 1998; McHugh et al., 1996). We, therefore, studied the place cell activity of CA1 neurons in DNRAb+ mice ($n = 8$) and DNRAb− mice ($n = 7$), prior to LPS administration and at various post-LPS time points (1, 2, 3, 4, 8, and 9 weeks). Using multi-electrode arrays directed to dorsal CA1 (Fig. 4A), we recorded both single neuron activity and local field potentials in freely moving mice within a square chamber. Because certain parameters of place cells can vary along the hippocampal proximal–distal axis (Henriksen et al., 2010), we ensured that electrode positions were comparable across all the recorded mice.

Theta rhythm was not affected by DNRAb exposure (Fig. 4B and C), demonstrating that the surviving CA1 neurons remained capable of engaging in normal local field potential activity. Prior to LPS exposure, place cells of DNRAb+ and DNRAb− mice had comparable place field sizes (Fig. 4D). At 1 week post-LPS, place field size was increased in neurons of both DNRAb+ and DNRAb− mice. However, by 2 weeks post-LPS, DNRAb+ place cells showed even larger place field sizes compared to pre-LPS values, while cells not exposed to DNRAb exhibited no change in place field size from baseline (Fig. 4D–F). The expanded place fields in hippocampal neurons of DNRAb+ mice were sustained up to 9 weeks (Fig. 4E). Importantly, the peak firing rates of DNRAb+ place

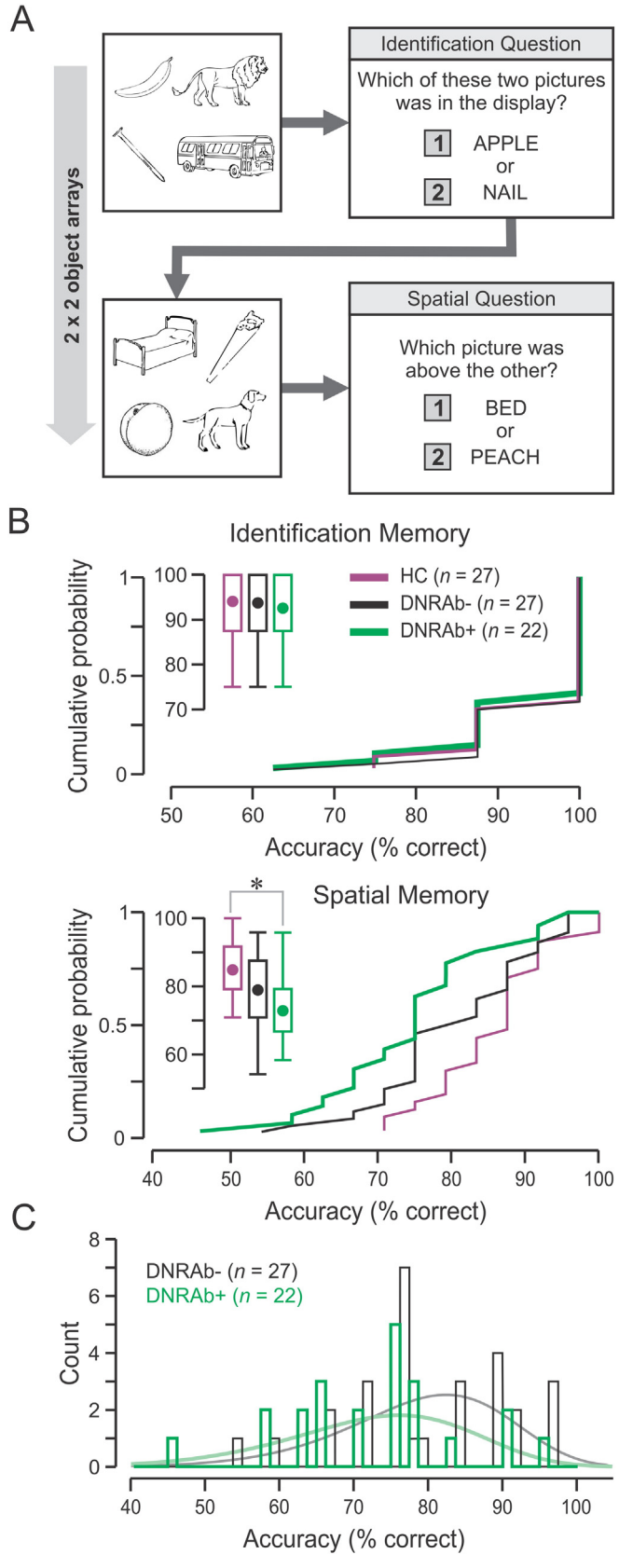

Fig. 1. Selective impairment of spatial memory in SLE patients with DNRAbs. (A) Schematic of the task with drawings of objects presented as 2 × 2 arrays for 6 s, followed immediately by an identification question or a spatial question. Subjects chose their answer by pressing a numeric keyboard. (B) Accuracy of responses, plotted as distributions of cumulative probabilities and box plots (insets, center dots represent the mean response), reveal no significant differences between groups in the identification memory component of the task (*top*) but marked differences between healthy controls (HC) and the DNRAb+ patients in the spatial memory component (*bottom*); * $P < 0.05$, *t* test. (C) Histograms for the accuracy of spatial memory reveal that the DNRAb+ group shows a clear distribution shift toward lower accuracy values ($\chi 2 = 2.93$, $P = 0.08$, Kruskal–Wallis ANOVA), which becomes significant if the worst performer in the DNRAb− group is ignored ($P < 0.05$, KWANOVA); n = number of subjects.

Please cite this article as: Chang, E.H., et al., Selective Impairment of Spatial Cognition Caused by Autoantibodies to the N-Methyl-D-Aspartate Receptor, EBioMedicine (2015), http://dx.doi.org/10.1016/j.ebiom.2015.05.027

cells were not different between the pre-LPS and 8-week post-LPS time points ($t = 0.53$, $P = 0.59$, t test), suggesting that the field size expansion was not due to a post-LPS decrease in peak firing rate, which would have allowed more pixels to be included in the definition of a field, thereby enlarging its size. Analysis of spatial information, a measure of how well the firing of place cells predicts the animal's location in space, was significantly decreased in the post-LPS period for DNRAb+ mice (Fig. S1). Thus,

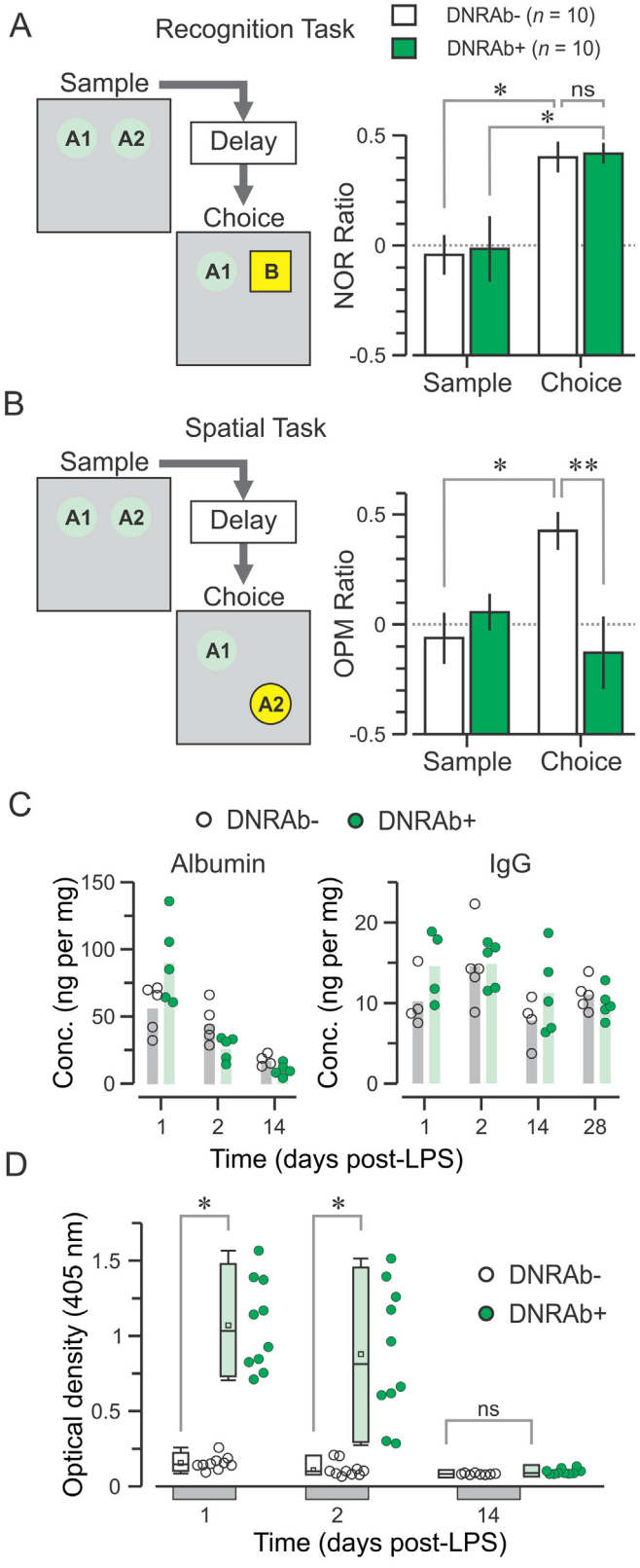

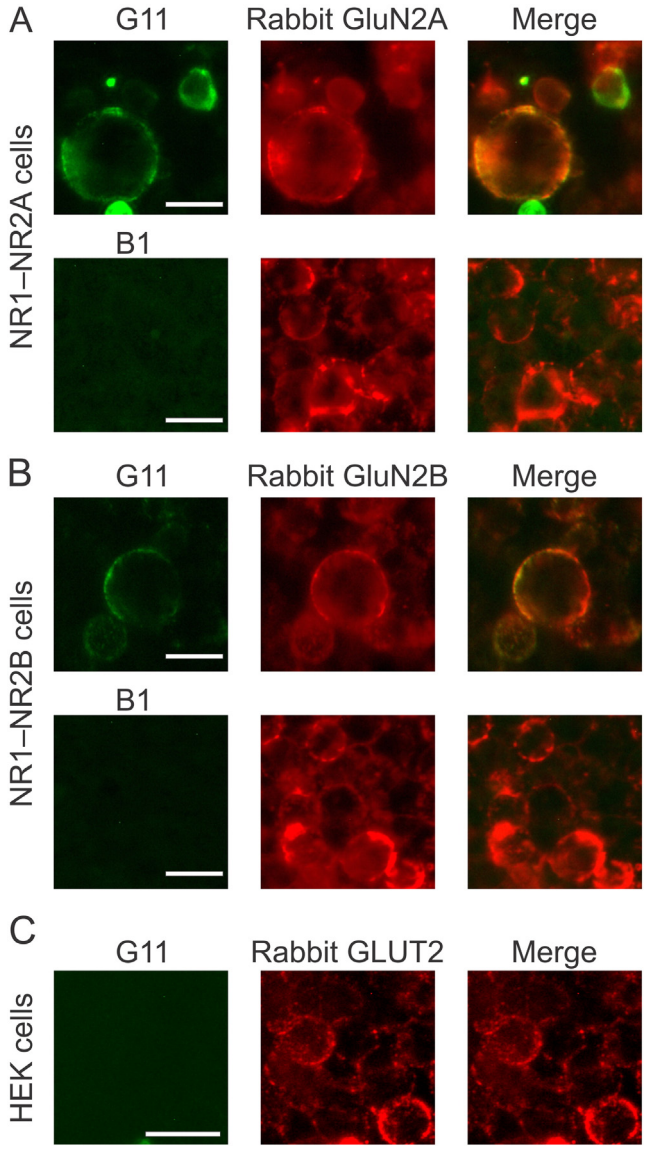

Fig. 3. DNRAbs bind to NMDARs expressed in the cell membrane. The panels show the binding of G11 (human monoclonal DNRAb cloned from a SLE patient) to transfected HEK-293 T cells. (A) *Left*, GluN1–GluN2A double transfected cells show clear surface binding of G11 (top, green signal, Alexa 488) but not B1, the control human antibody without NMDAR binding (bottom). *Middle*, strong binding of rabbit anti-GluN2A antibody to surface-expressed GluN2A (red signal, Alexa 594). *Right*, merged signal indicates that G11 binds to the GluN2A-containing NMDARs. (B) GluN1–GluN2B double transfected cells show a similar binding pattern for the GluN2B-containing NMDARs. (C) Binding of G11 to rabbit polyclonal antibodies was excluded by demonstrating that G11 does not bind to the cell surface of HEK-293 T cells incubated with rabbit polyclonal GLUT2 antibody, which abundantly binds to the cell surface of HEK-293 T cells (red staining). Bar, 30 μm. (For interpretation of the references to color in this figure legend, the reader is referred to the web version of this article.)

Fig. 2. Mice with hippocampal exposure to DNRAbs show impaired spatial memory but normal object recognition. (A) *Left*, schematic of the novel object recognition (NOR) task comprising sample (5 min), delay (10 min), and choice (5 min) phases. A1 and A2 represent identical objects, whereas B refers to a novel object. *Right*, both groups displayed a robust bias for exploring the novel object during the choice phase. Data are mean ± SEM. (B) *Left*, schematic of the object place memory (OPM) task with sample (5 min), delay (10 min), and choice (5 min) in which the A2 object is moved to a different location. *Right*, DNRAb− mice explored the moved object preferentially, while DNRAb+ mice did not. Data are mean ± SEM. (C) *Left*, concentration (conc.) of albumin within the hippocampus, extracted at 1, 2 or 14 days post-LPS. *Right*, IgG concentration at different points after LPS treatment. Bars represent the mean values. (D) Box plots for the titer of DWEYS-binding antibody expressed as optical density; ns, non-significant; * $P < 0.05$, ** $P < 0.01$, t test.

Please cite this article as: Chang, E.H., et al., Selective Impairment of Spatial Cognition Caused by Autoantibodies to the N-Methyl-D-Aspartate Receptor, EBioMedicine (2015), http://dx.doi.org/10.1016/j.ebiom.2015.05.027

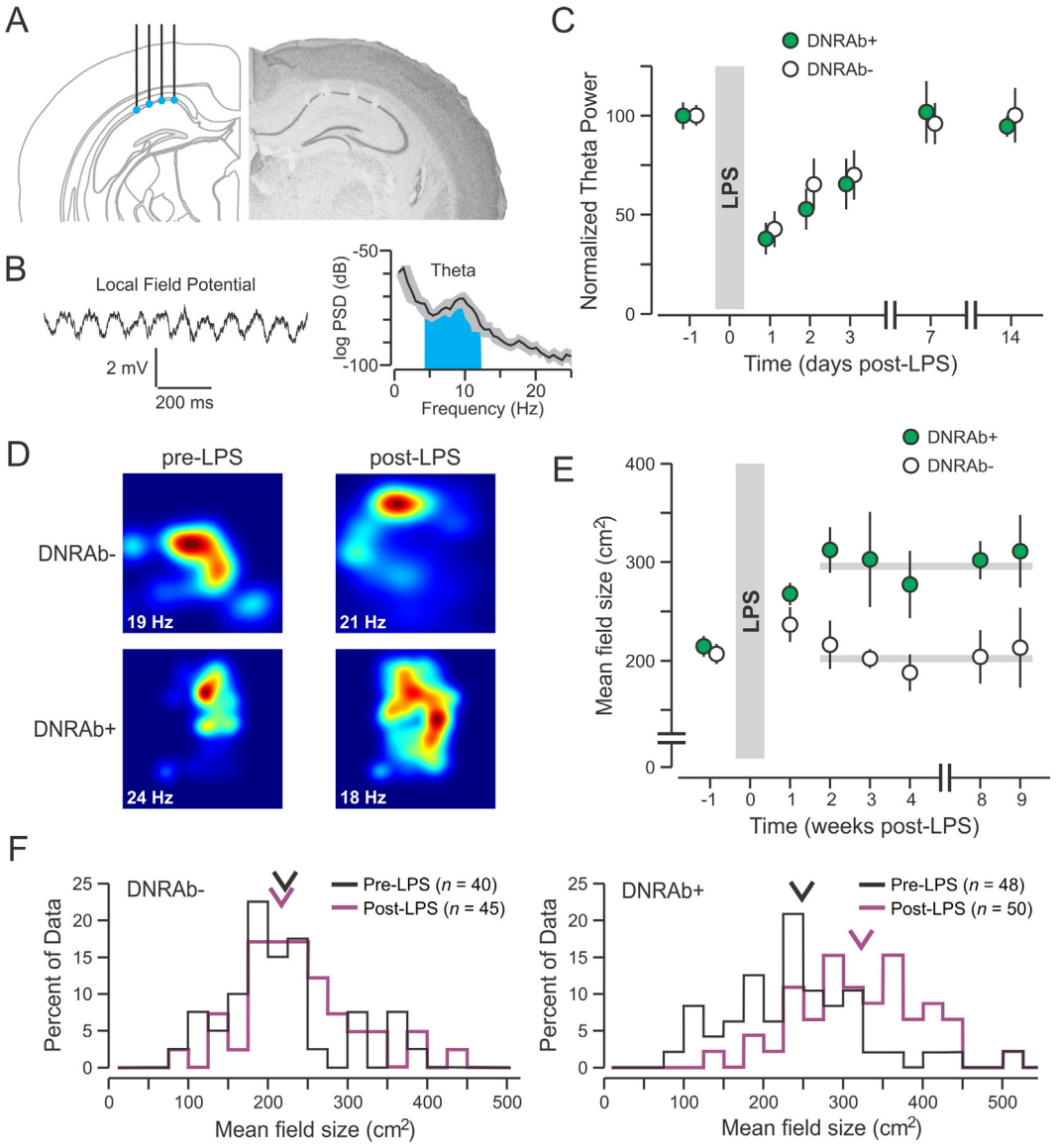

Fig. 4. Place cells in the CA1 hippocampal region of mice with hippocampal exposure to DNRAbs show abnormally large place fields. (A) *Left*, schematic view of the placement of the multi-electrode array in the dorsal CA1 region. *Right*, representative Nissl-stained section showing the lesions of the electrode tips in the cell body layer of CA1. (B) *Left*, representative local field potentials from one of the electrodes displaying an oscillatory episode. *Right*, plot of power spectral density obtained from the local field potentials, indicating the band for theta frequency (4–12 Hz, cyan). (C) Time course for the power of theta rhythm (mean ± SEM) reveals no differences between DNRAb+ and DNRAb− groups, up to 2 weeks post-LPS when values return to baseline ($F = 1.68$, $P = 0.25$, ANOVA with repeated measures). (D) Representative firing rate maps, recorded 1 week pre-LPS and 4 weeks post-LPS, during 10-min sessions in an arena (viewed from the top, 40 cm on the side). Color scale indicates frequency (Hz, spikes per second), in which red corresponds to the peak firing rate (numbers at lower left of each panel) and blue to null firing. (E) Time course of place field sizes (mean ± SEM) reveals a permanent enlargement in DNRAb+ mice, up to 9 weeks post-LPS. ANOVA, for the post-LPS points, shows that the groups are significantly different ($F = 27.11$, $P < 0.0001$). (F) Histograms for place field sizes of all place cells recorded in the pre-LPS and post-LPS periods. The DNRAb+ group shows a significant distribution shift toward larger field size values ($D = 0.45$, $P < 0.0001$, Kolmogorov–Smirnov test); n indicates number of cells. (For interpretation of the references to color in this figure legend, the reader is referred to the web version of this article.)

exposure to DNRAbs led to a persistent expansion of place fields that evolved even as DNRAbs were no longer present in the hippocampus, and the reduced information content of post-LPS place cells in DNRAb+ mice could ultimately result in a depreciated spatial map.

3.4. Altered Dendritic Branching in Pyramidal Cells of DNRAb + Mice

NMDARs are located primarily within the dendritic spines of neurons. Decreases in the density of dendritic spines of hippocampal neurons have been correlated with defective memory (Fiala et al., 2002). To study if the functional impairment we observed in CA1 neurons correlated with structural lesions in dendrites, we assessed the number of branches emanating from individual CA1 pyramidal neurons using Scholl analysis (Fig. 5A). There was a loss of dendritic branches in the DNRAb+ group that became evident between 2 and 8 weeks post-LPS, compared to neurons of DNRAb− mice (Fig. 5B). We also examined dendritic processes in CA3 neurons, which project to CA1 neurons, and again found a loss of branches in DNRAb+ compared to DNRAb− mice (Fig. 5C). This was a regionally restricted abnormality as neurons in layer 4 of the parietal association cortex (Fig. 5C) and in the anterior basolateral amygdala (data not shown) exhibited similar dendritic branching in both cohorts. We next assessed the density of dendritic spines in the apical dendrites of CA1 pyramidal cells (*stratum radiatum* and *stratum lacunosum moleculare*) and found significantly fewer spines in DNRAb+ compared to DNRAb− mice (Fig. 5D). Thus, DNRAb exposure caused a sustained morphologic change in hippocampal CA1 and CA3 neurons providing a structural correlate for the enlarged place field size and the impaired spatial memory.

Please cite this article as: Chang, E.H., et al., Selective Impairment of Spatial Cognition Caused by Autoantibodies to the N-Methyl-D-Aspartate Receptor, EBioMedicine (2015), http://dx.doi.org/10.1016/j.ebiom.2015.05.027

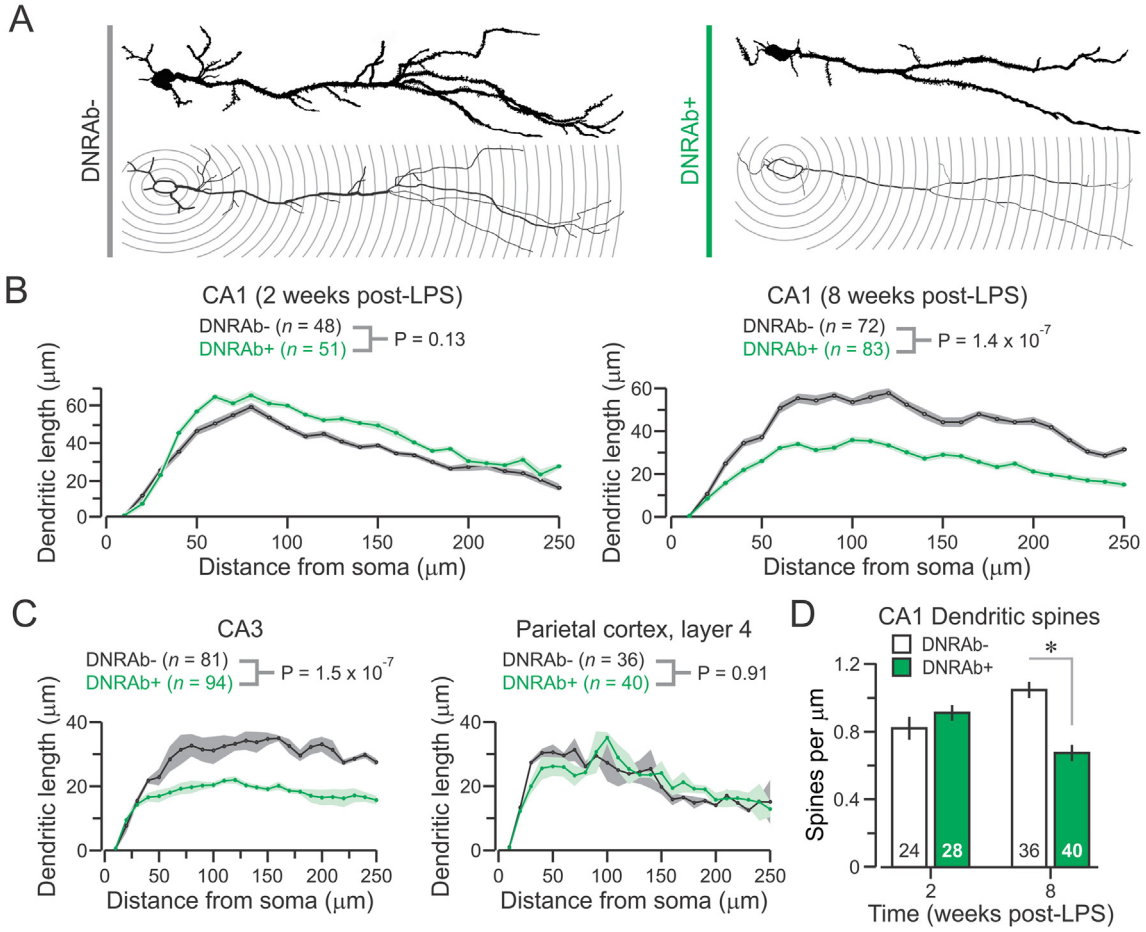

Fig. 5. Pyramidal neurons of mice with hippocampal exposure to DNRAbs show abnormal dendritic branching and spine density. (A) Traced drawings of representative Golgi-impregnated CA1 pyramidal neurons from DNRAb− (*left*) and DNRAb+ (*right*) mice. (B) Scholl analysis depicts dendritic length as a function of distance from the soma. *Left*, both groups of mice have comparable dendritic length at 2 weeks post-LPS ($t = 0.5$, $P = 0.13$, t test). *Right*, the DNRAb+ neurons have significant dendritic loss at 8 weeks post-LPS ($t = 7.9$, $P < 0.0001$, t test); n = number of cells; 3 animals per group. (C) *Left*, CA3 pyramidal cells show significant loss of dendritic branches in the DNRAb+ group at 8 weeks post-LPS ($t = 7.1$, $P < 0.0001$, t test). *Right*, neurons in the layer 4 of the parietal cortex have similar dendritic length in both groups at 8 weeks post-LPS ($t = 0.01$, $P = 0.9$, t test); n = number of cells; 3 animals per group. (D) Density of synaptic dendritic spines (mean ± SEM) in CA1 neurons is comparable for both groups at 2 weeks post-LPS ($t = 0.05$, $P = 0.6$, t test) but by 8 weeks post-LPS, the spine count in the DNRAb+ mice is significantly reduced ($t = 7.86$, $P < 0.0001$, t test); numbers in bars indicate dendritic trees counted; 3 animals per group.

4. Discussion

This study shows that SLE patients carrying circulating DNRAbs display a selective impairment in spatial cognition. While SLE patients commonly complain of problems with spatial navigation, such as not knowing whether they are moving toward or away from home, or not knowing if they are on their block or a block away, this study is unique in that spatial performance has been explicitly tested and has been related to serology. Previous studies have demonstrated that DNRAbs can be found in the CSF of SLE patients at concentrations capable of altering the strength of murine NMDAR-mediated synaptic potentials and causing excitotoxic neuronal death in mice in vivo, or death of human NMDAR-expressing cell lines (DeGiorgio et al., 2001; Faust et al., 2010; Fragoso-Loyo et al., 2008). Moreover, DNRAbs in the CSF have been strongly associated with non-focal CNS disease (Arinuma et al., 2008; Fragoso-Loyo et al., 2008; Gono et al., 2011; Yoshio et al., 2006), while neuroimaging and neuropathologic studies of SLE patients have identified the hippocampus as a region of frequent abnormality (Appenzeller et al., 2006; Ballok et al., 2004).

This study shows that mice in which DNRAbs penetrate into the hippocampus display a clear disruption in the CA1 place cell system, which is a key part of the neural substrate for spatial navigation (O'Keefe, 2007). Also, some crucial properties of place cells are NMDAR-dependent (Ekstrom et al., 2001; Kentros et al., 1998). Importantly, the significant DNRAb-mediated expansion in place field size of CA1 neurons likely leads to a spatial map with lower resolution. Similar alterations in place cell firing have been described in a mouse model of Alzheimer's disease (Cacucci et al., 2008), as well as mice with a hippocampal-specific deletion of the gene encoding GluN1 (McHugh et al., 1996). Since NMDARs are located in dendritic spines, we also analyzed CA1 dendrites and confirmed reduced number of dendritic branches and dendritic spines in CA1 neurons. A similar abnormality was seen in the CA1-projecting CA3 neurons that may reflect direct exposure to DNRAbs or alternatively, retrograde damage to the Schaffer commissural collateral CA3 axons that project to CA1 neurons (Wang et al., 2012). Surprisingly, both functional and structural neuronal damage evolved after the inciting trigger was no longer present, and persisted for at least 2 months after the BBB breach. This slow evolution of dysfunction is consistent with the clinical data on NPSLE. Changes in cognitive function are insidious and most commonly do not occur concurrent with flares in disease activity or with overt evidence of CNS inflammation (Shimojima et al., 2005).

SLE-prone mice, such as the NZB/W and MRL/lpr strains, have been previously studied and show a marked impairment in spatial memory that develops once both autoantibodies and inflammatory cytokines are elevated (Sakic, 2012). Thus, the contribution of a specific antibody subset cannot be assessed in these mice. We found that mice with hippocampal exposure to DNRAbs were not impaired in the NOR task. By contrast, hippocampal exposure to DNRAbs correlates with spatial memory impairment in four distinct assessments: the T-maze, the

Please cite this article as: Chang, E.H., et al., Selective Impairment of Spatial Cognition Caused by Autoantibodies to the N-Methyl-D-Aspartate Receptor, EBioMedicine (2015), http://dx.doi.org/10.1016/j.ebiom.2015.05.027

Morris water maze, the clock maze, reported previously (Kowal et al., 2004, 2006), and the OPM task described here. Since SLE patients carrying elevated titers of DNRAbs exhibited impaired spatial memory compared to HC subjects, the mouse model appears to be a valid model for NPSLE. Changes in dendritic complexity in hippocampal neurons have been reported in a model of anti-phospholipid syndrome, although the mechanism for neuronal destruction in unknown (Frauenknecht et al., 2014). There are numerous brain-reactive antibodies in SLE (Yaniv et al., 2015). It will be important to determine how each might contribute to manifestations of NPSLE.

Several reports have implicated antibodies that react with the NMDAR in limbic encephalitis characterized by psychosis, seizures and diminished wakefulness (Dalmau et al., 2011). The antibodies associated with this condition bind to the GluN1 subunit, do not cross react with DNA, and cause receptor internalization *in vitro*. Whether the decreased density of NMDAR that can be induced *in vitro* by the GluN1 binding-antibodies also occurs *in vivo* and whether this relates to the clinical symptoms remain open questions. Interestingly, these ant-GluN1 antibodies can be found in 10% of healthy individuals (Hammer et al., 2014). Moreover, studies in which these antibodies were transferred into mice show they cause no brain injury unless there is a loss of BBB integrity (Hammer et al., 2014). This model is therefore, comparable to our own except that anti-NMDAR antibodies binding to the GluN1 subunit cause seizures and affect imbalance rather than cognitive disorders in mice.

These results extend our mouse model of DNRAb-mediated brain dysfunction, and validate its utility as a model of NPSLE. The murine studies allowed us to pursue an understanding of DNRAb-mediated changes in neuronal physiology and structure that is not accessible in human studies, such as post-mortem analyses of brain pathology, as many additional brain insults may contribute to post-mortem pathology. Our study provides the insight that DNRAb-mediated damage is an evolving process that involves both functional and structural changes in surviving neurons, and suggests that there may be a therapeutic window that is longer than the period of BBB compromise. It remains to future studies to determine if the pathology reflects neuron-intrinsic events secondary to DNRAb exposure or is a consequence of microglia activation. Furthermore, by utilizing a psychometric task, we show that DNRAb+ patients exhibit a selective impairment in recalling spatial relations. The identification of pathogenic mechanisms and appropriate neuropsychiatric assessments through the exploration of models such as ours is key to designing strategies for neuroprotection in NPSLE patients.

Research in context

Chang et al. show that DNRAbs, lupus antibodies that bind DNA and the GluN2A–GluN2B subunits of NMDAR, cause selective impairment of spatial memory in patients and mice. Mouse studies reveal structural and functional deficiencies in CA1 place cells that might represent the neural correlate of the spatial impairment.

Acknowledgments

We thank Sylvia Jones for assistance in manuscript preparation, and Kevin Tracey and Jeffrey Ravetch for suggestions. This research was funded by NIH grant P01-AI073693 (to B.D., P.H., M.M., B.V.) and NIH grant P01-AI102852 (to B.D., P.H., B.V.). The contents are solely the responsibility of the authors and do not necessarily represent the official views of the NIH. Funding sources did not have any involvement in study design, data analysis, and interpretation of results.

Appendix A. Supplementary data

Supplementary data to this article can be found online at http://dx.doi.org/10.1016/j.ebiom.2015.05.027.

References

American College of Rheumatology, 1999. The American College of Rheumatology nomenclature and case definitions for neuropsychiatric lupus syndromes. Arthritis Rheum. 42, 599–608.
Appenzeller, S., Carnevalle, A.D., Li, L.M., Costallat, L.T., Cendes, F., 2006. Hippocampal atrophy in systemic lupus erythematosus. Ann. Rheum. Dis. 65, 1585–1589.
Appenzeller, S.F., Cendes, F., Costallat, L.T., 2009. Cognitive impairment and employment status in systemic lupus erythematosus: a prospective longitudinal study. Arthritis Rheum. 61, 680–687.
Arinuma, Y., Yanagida, T., Hirohata, S., 2008. Association of cerebrospinal fluid anti-NR2 glutamate receptor antibodies with diffuse neuropsychiatric systemic lupus erythematosus. Arthritis Rheum. 58, 1130–1135.
Ballok, D.A., Woulfe, J., Sur, M., Cyr, M., Sakic, B., 2004. Hippocampal damage in mouse and human forms of systemic autoimmune disease. Hippocampus 14, 649–661.
Cacucci, F., Yi, M., Wills, T.J., Chapman, P., O'Keefe, J., 2008. Place cell firing correlates with memory deficits and amyloid plaque burden in Tg2576 Alzheimer mouse model. Proc. Natl. Acad. Sci. U. S. A. 105, 7863–7868.
Chang, E.H., Huerta, P.T., 2012. Neurophysiological correlates of object recognition in the dorsal subiculum. Front. Behav. Neurosci. 6, 46.
Dalmau, J., Lancaster, E., Martinez-Hernanez, E., Rosenfeld, M.R., Balice-Goron, R., 2011. Clinical experience and laboratory investigations with anti-NMDAR encephalitis. Lancet Neurol. 10, 63–74.
DeGiorgio, L.A., Konstantinov, K.N., Lee, S.C., Hardin, J.A., Volpe, B.T., Diamond, B., 2001. A subset of lupus anti-DNA antibodies cross-reacts with the NR2 glutamate receptor in systemic lupus erythematosus. Nat. Med. 7, 1189–1193.
Diamond, B., Honig, G., Mader, S., Brimberg, L., Volpe, B.T., 2013. Brain-reactive antibodies and disease. Annu. Rev. Immunol. 31, 345–385.
Ekstrom, A.D., Meltzer, J., McNaughton, B.L., Barnes, C.A., 2001. NMDAR antagonism blocks experience-dependent expansion of hippocampal place cells. Neuron 31, 631–638.
Faust, T.W., et al., 2010. Neurotoxic lupus autoantibodies alter brain function through two distinct mechanisms. Proc. Natl. Acad. Sci. U. S. A. 107, 18569–18574.
Faust, T.W., Robbiati, S., Huerta, T.S., Huerta, P.T., 2013. Dynamic NMDAR-mediated properties of place cells during the object place memory task. Front. Behav. Neurosci. 7, 202.
Fiala, J.C., Spacek, J., Harris, K.M., 2002. Dendritic spine pathology: cause or consequence of neurological disorders? Brain Res. Rev. 39, 29–54.
Fragoso-Loyo, H., et al., 2008. Serum and cerebrospinal fluid autoantibodies in patients with neuropsychiatric lupus erythematosus. Implications for diagnosis and pathogenesis. PLoS One 3, e3347.
Frauenknecht, K., Katzav, A., Weiss Lavi, R., Sabag, A., Otten, S., Chapman, J., Sommer, C.J., 2014. Mice with experimental antiphospholipid syndrome display hippocampal dysfunction and a reduction of dendritic complexity in hippocampal CA1 neurones. Neuropathol. Appl. Neurobiol. http://dx.doi.org/10.1111/nan.12180 (Sep 9, Epub ahead of print).
Gladman, D.D., et al., 1997. The reliability of the Systemic Lupus International Collaborating Clinics/American College of Rheumatology Damage Index in patients with systemic lupus erythematosus. Arthritis Rheum. 40, 809–813.
Gono, T., Kawaguchi, Y., Kaneko, H., Nishimura, K., Hanaoka, M., Kataoka, S., Okamoto, Y., Katsumata, Y., Yamanaka, H., 2011. Anti-NR2A antibody as a predictor for neuropsychiatric systemic lupus erythematosus. Rheumatology 50, 1578–1585.
Hammer, C., et al., 2014. Neuropsychiatric disease relevance of circulating anti-NMDA receptor autoantibodies depends on blood–brain barrier integrity. Mol. Psychiatry 19, 1143–1149.
Hanly, J.G., McCurdy, G., Fougere, L., Douglas, J.A., Thompson, K., 2004. Neuropsychiatric events in systemic lupus erythematosus: attribution and clinical significance. J. Rheumatol. 31, 2156–2162.
Henriksen, E.J., Colgin, L.L., Barnes, C.A., Witter, M.P., Moser, M.B., Moser, E.I., 2010. Spatial representation along the proximodistal axis of CA1. Neuron 68, 127–137.
Hirohata, S., Arinuma, Y., Yanagida, T., Yoshio, T., 2014. Blood–brain barrier damages and intrathecal synthesis of anti-N-methyl-D-aspartate receptor NR2 antibodies in diffuse psychiatric/neuropsychological syndromes in systemic lupus erythematosus. Arthritis Res. Ther. 16, R77.
Kentros, C., Hargreaves, E., Hawkins, R.D., Kandel, E.R., Shapiro, M., Muller, R.V., 1998. Abolition of long-term stability of new hippocampal place cell maps by NMDA receptor blockage. Science 280, 2121–2126.
Kowal, C., DeGiorgio, L.A., Nakaoka, T., Hetherington, H., Huerta, P.T., Diamond, B., Volpe, B.T., 2004. Cognition and immunity; antibody impairs memory. Immunity 21, 179–188.
Kowal, C., DeGiorgio, L.A., Lee, J.Y., Edgar, M.A., Huerta, P.T., Volpe, B.T., Diamond, B., 2006. Human lupus autoantibodies against NMDA receptors mediate cognitive impairment. Proc. Natl. Acad. Sci. U. S. A. 103, 19854–19859.
Laflamme, N., Soucy, G., Rivest, S., 2001. Circulating cell wall components derived from gram-negative, not gram-positive, bacteria cause a profound induction of the gene-encoding Toll-like receptor 2 in the CNS. J. Neurochem. 79, 648–657.
Lauvsnes, M.B., Omdal, R., 2012. Systemic lupus erythematosus, the brain, and anti-NR2 antibodies. J. Neurol. 259, 622–629.
Mader, S., et al., 2010. Patterns of antibody binding to aquaporin-4 isoforms in neuromyelitis optica. PLoS One 5, e10455.
McHugh, T.J., Blum, K.I., Tsien, J.Z., Tonegawa, S., Wilson, M.A., 1996. Impaired hippocampal representation of space in CA1-specific NMDAR1 knockout mice. Cell 87, 1339–1349.
Nowicka-Sauer, K., Czuszynska, Z., Smolenska, Z., Siebert, J., 2011. Neuropsychological assessment in systemic lupus erythematosus patients: clinical usefulness of first-choice diagnostic tests in detecting cognitive impairment and preliminary diagnosis of neuropsychiatric lupus. Clin. Exp. Rheumatol. 29, 299–306.

Please cite this article as: Chang, E.H., et al., Selective Impairment of Spatial Cognition Caused by Autoantibodies to the N-Methyl-D-Aspartate Receptor, EBioMedicine (2015), http://dx.doi.org/10.1016/j.ebiom.2015.05.027

O'Keefe, J., 2007. Hippocampal neurophysiology in the behaving animal. In: Andersen, P., Morris, R.M., Amaral, D., Bliss, T., O'Keefe, J. (Eds.), The Hippocampus Book. Oxford University Press, New York, NY, pp. 475–548.
Paoletti, P., 2011. Molecular basis of NMDA receptor functional diversity. Eur. J. Neurosci. 33, 1351–1365.
Petri, M., Buyon, J., Kim, M., 1999. Classification and definition of major flares in SLE clinical trials. Lupus 8, 685–691.
Sakic, B., 2012. The MRL model: an invaluable tool in studies of autoimmunity–brain interactions. Methods Mol. Biol. 934, 277–299.
Shimojima, Y., Matsuda, M., Gono, T., Ishii, W., Ikeda, S., 2005. Relationship between clinical factors and neuropsychiatric manifestations in systemic lupus erythematosus. Clin. Rheumatol. 24, 469–475.
Skaggs, W.E., McNaughton, B.L., Gothard, K.M., Markus, E.J., 1993. An information–theoretic approach to deciphering the hippocampal code. Neural Inf. Process. Syst. 5, 1030–1037.
Toledano, P., Sarbu, N., Espinosa, G., Bargallo, N., Cervera, R., 2013. Neuropsychiatric systemic lupus erythematosus: magnetic resonance imaging findings and correlation with clinical and immunological features. Autoimmun. Rev. 12, 1166–1170.
Tsokos, G.C., 2011. Systemic lupus erythematosus. N. Engl. J. Med. 365, 2110–2121.
Wang, J.T., Medress, Z.A., Barres, B.A., 2012. Axon degeneration: molecular mechanisms of a self-destruction pathway. J. Cell Biol. 196, 7–18.
Yaniv, G., et al., 2015. A volcanic explosion of autoantibodies in systemic lupus erythematosus: a diversity of 180 different antibodies found in SLE patients. Autoimmun. Rev. 14, 75–79.
Yoshio, T., Onda, K., Nara, H., Minota, S., 2006. Association of IgG anti-NR2 glutamate receptor antibodies in cerebrospinal fluid with neuropsychiatric systemic lupus erythematosus. Arthritis Rheum. 54, 675–678.

Please cite this article as: Chang, E.H., et al., Selective Impairment of Spatial Cognition Caused by Autoantibodies to the N-Methyl-D-Aspartate Receptor, EBioMedicine (2015), http://dx.doi.org/10.1016/j.ebiom.2015.05.027